J Therm Anal Calorim (2010) 99:791–797
DOI 10.1007/s10973-009-0438-0

Modelling of the thermal effects involved in the determination of heat of mixing, using an ITC operating in continuous mode

M. Rodríguez de Rivera · F. Socorro · J. S. Matos

MEDICTA2009 Conference

Abstract A simplified RC model which simulates the operation mode of an isothermal titration calorimeter (ITC), when it is used in a continuous mode to determine heat of mixing, is proposed. The model takes into account several thermal effects that are evident in the mixing process and it must be identified and quantified to determine reliable values of heat of mixing. The main effects considered in the development of the model were those caused by: (i) the difference between the temperatures of the injected liquid and the mixture, (ii) the increase in heat capacity of the mixture and the thermal conductance of the couplings between the mixture and its surroundings and (iii) the changes in the power dissipated by stirring after injection. A good agreement between model and experimental results is observed.

Keywords Calorimetric model · Calorimetric simulation · Excess molar enthalpies · Isothermal titration calorimeter

Introduction

The isothermal titration calorimeters (ITC) can be used for the analysis of solid–liquid and liquid–liquid processes, and they allow the determination of enthalpies of solution, enthalpies of dilution, enthalpies of reaction in solution, enthalpies of mixing, etc. The standard operation mode to obtain heat of mixing of liquid mixtures is to inject a known amount of a liquid on another liquid. The mixing process produces a calorimetric signal which returns to the experimental zero (baseline). The heat of mixing can be then obtained by integration of the calorimetric signal (in mV) and dividing the area obtained for the sensitivity of the calorimeter (in mV W^{-1}). This process is repeated until the volume of the mixing cell has been completed.

On the other hand, the adequate determination of heat of mixing using an ITC supposed to evaluate all the thermal effects associated with both the experimental device and the working method. We have observed the presence of various thermal effects added to the heat of mixing. These effects are explained below:

(i) The difference between the temperatures of the injected liquid and the mixture. This fact gives rise to an additional power associated to the heating or cooling of the injected liquid (depending on whether the mixture is exothermic or endothermic). This power is proportional both to the injection flow and the heat capacity of the injected liquid [1–3].

(ii) The increasing in the heat capacity of the mixture and the thermal conductance of the couplings between the liquid mixture and its surroundings when the volume of liquid in the mixture cell increases. This fact leads to modifications, both in the static response (sensitivity) and in the dynamic response (time constants) of the calorimetric system [4].

(iii) The changes in the power dissipated (by stirring) due to the changes in density and viscosity of the mixture when the liquid is injected. These changes produce alterations in the baseline, which may be relatively important [5, 6].

(iv) The small differences obtained for the sensitivity of the calorimeter when the Joule dissipation and mixture dissipations are produced. These differences

M. Rodríguez de Rivera (✉) · F. Socorro · J. S. Matos
Departamento de Física, Universidad de Las Palmas de Gran Canaria, 35017 Las Palmas de Gran Canaria, Spain
e-mail: mrodriguez@dfis.ulpgc.es

are closely related to the fact that both energetic processes occur at different locations [7].

In order to evaluate the effects mentioned earlier, we have simulated the operation mode of the calorimeter using a simplified RC model for three domains. The model is obtained from experimental measurements made in a Calorimeter TAM2277-201/2250 by Thermometric. The modelling can assess the impact that these effects have on the calorimetric signal and/or the thermodynamic result, and, therefore, it makes the necessary corrections in each situation.

Experimental device and model

The instrument used in this study was an ITC TAM2277-201/2250 by Thermometric AB using the stirrer recommended by the manufacturer for this experimental device. Mixing cells of 5 mL capacity were used, although the recommended maximum volume of liquid is 2.5 mL [8]. The calorimetric signal is directly read using a HP3457A digital multimeter (±10 nV). The calibration of the device has been described in a previous work [7], and the sensitivity obtained was 391 ± 9 mV W^{-1}. In the chemical calibrations, the water + ethanol and cyclohexane + benzene binary systems were used.

In order to reproduce the experimental facts mentioned above (for the simplest possible way) we used the localized constants model (RC model) which has been frequently used to simulate the operation mode of several conduction calorimeters [9–14]. The identification of the experimental curves from electrical calibrations resulted in transfer functions (TF) with two time constants. However, the different values obtained for the sensitivity, taken from electrical and chemical calibrations, suggest the creation of a specific domain for each source of energy dissipation. For this reason, we chose a model of three domains (Fig. 1), where the first one represents the place where the liquid mixture occurs, the second one represents the area where the Joule dissipation is produced, and the third one represents the container recipient. Each domain has a heat capacity C_i, and the thermal coupling between adjacent domains is characterized by the thermal conductance P_{ik} (the thermal conductance, in W K^{-1}, is the reciprocal of the thermal resistance R_{ik}). The calculation of the P_{ik} values has been described in detail in [9, 13].

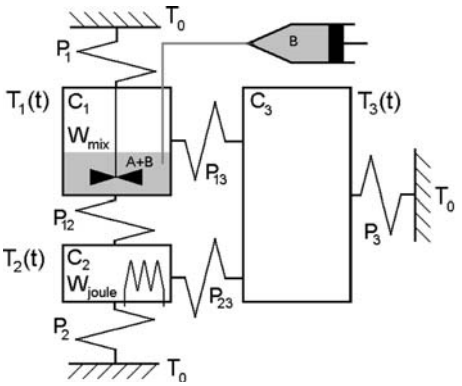

Fig. 1 Diagram for the RC model chosen

The development of the model requires an energy balance for each domain. Assuming that the power generated or absorbed in the domain of capacity C_i is the sum of the stored power in itself, $C_i(\mathrm{d}T_i/\mathrm{d}t)$, plus those transmitted by conduction to the thermostat (T_0) and the neighbouring domains, we obtain the following model:

$$\begin{aligned} &W_{\mathrm{mix}} + W_{\mathrm{stirring}} + \rho c_p f(T_0 - T_1) \\ &= C_1 \frac{\mathrm{d}T_1}{\mathrm{d}t} + P_{12}(T_1 - T_2) + P_{13}(T_1 - T_3) \\ &\quad + P_{10}(T_1 - T_0) \\ &W_{\mathrm{elect}} = C_2 \frac{\mathrm{d}T_2}{\mathrm{d}t} + P_{12}(T_2 - T_1) + P_{23}(T_2 - T_3) \\ &\quad + P_{20}(T_2 - T_0) \\ &0 = C_3 \frac{\mathrm{d}T_3}{\mathrm{d}t} + P_{13}(T_3 - T_1) + P_{23}(T_3 - T_2) \\ &\quad + P_{30}(T_3 - T_0). \end{aligned} \tag{1}$$

For the first domain, we consider the mixing power (W_{mix}) and the power dissipated by stirring (W_{stirring}) and for the second one, the power dissipated in the electrical calibrations (W_{elect}). The power associated to the heating or cooling of the injected fluid, when its temperature changes from T_0 (temperature of the thermostat) to T_1 (temperature of the mixture), is also incorporated in the equation for the first domain. This power is represented by $\rho c_p f(T_0–T_1)$, where ρc_p is the volumetric heat capacity of injected liquid and f is the injection flow. Furthermore, because of the fact that the third domain is in contact with the detector system (thermocouples), we make the calorimetric signal, $y(t)$, to be proportional to the difference between the temperatures of the thermostat and the third domain, i.e.,

$$y(t) = k_{\mathrm{T}}(T_3 - T_0). \tag{2}$$

On the other hand, if we consider the calorimetric device as a two input–one output system, we can relate the Laplace transforms of the inputs and the Laplace transform of the output through TF. In the calculations, the power dissipated in the first and the second domains, $w_1(t)$ and $w_2(t)$, were the inputs and the calorimetric signal, $y(t)$, was the output. Additionally, to apply the Laplace transform to the previous system of equations (Eq. 1), it is necessary to assume that the C_i and P_{ik} values, corresponding to different levels of liquid in the cell mixing, do not vary with time. With these considerations, we obtain

$$
\begin{aligned}
Y(s) &= \frac{G_{\text{mix}}(s+s^*_{\text{mix}})}{(s+s_1)(s+s_2)(s+s_3)}W_1(s) \\
&+ \frac{G_{\text{Joule}}(s+s^*_{\text{Joule}})}{(s+s_1)(s+s_2)(s+s_3)}W_2(s) \\
&= \frac{K_{\text{mix}}(1+s\tau^*_{\text{mix}})}{(1+s\tau_1)(1+s\tau_2)(1+s\tau_3)}W_1(s) \\
&+ \frac{K_{\text{Joule}}(1+s\tau^*_{\text{Joule}})}{(1+s\tau_1)(1+s\tau_2)(1+s\tau_3)}W_2(s) \\
&= TF_1(s)W_1(s) + TF_2(s)W_2(s).
\end{aligned} \tag{3}
$$

In Eq. 3, $Y(s)$, $W_1(s)$ and $W_2(s)$ are the Laplace transforms of $y(t)$, $w_1(t)$ and $w_2(t)$, respectively, s_i and s_i^* are the poles and zeros for each TF; K_{mix} and K_{elect} are the sensitivities for each TF (TF_1 and TF_2) and $\tau_i = -1/s_i$, $\tau^* = -1/s^*$.

Identification of the model

The model parameters were optimized by minimizing the squared error between the experimental curves and those obtained by the equations of the model (Eq. 1). In this process, the simplex search algorithm method by Nelder and Mead [15] and the software MatLab [16] were used. The experimental curves used in the optimization process are shown in Fig. 2, where the first and last curves (J1 and J2) correspond to electrical calibrations (10 mW for 100 s). The remaining curves (M1–M10) correspond to successive injections of 0.1 mL of ethylene glycol on 1.5 mL of 2-pyrrolidone. Injection flow and stirring speed were 1 μL s^{-1} and 120 rpm, respectively.

Given that the objective is to find a model valid for the entire range of variation of the volume of liquid placed in the mixing cell, the identification process is done by

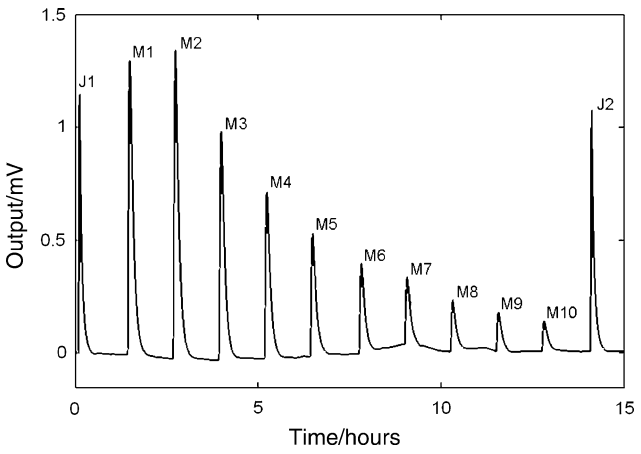

Fig. 2 Calorimetric curves used in the identification of the model. J1 and J2 are electrical calibrations. M1 to M10 correspond to successive injections of 0.1 mL of ethylene glycol (f = 1 μL s^{-1}) on 1.5 mL of 2-pyrrolidone

Table 1 Values of RC model (Eqs. 1 and 2)

RC model	$k_T = 0.0427$ mV K^{-1}	
C_1 (Table 2)	$C_2 = 2.045$ J K^{-1}	$C_3 = 17.586$ W K^{-1}
P_{10} (Table 2)	$P_{12} = 0.00482$ W K^{-1}	P_{13} (Table 2)
$P_{20} = 0.03279$ W K^{-1}	$P_{23} = 0.06672$ W K^{-1}	$P_{30} = 0.05747$ W K^{-1}

adjusting simultaneously the extreme calorimetric curves (J1, M1, M10 and J2) and an intermediate calorimetric curve (M5). In this process, the parameters C_2, C_3, P_{12}, P_{20}, P_{23}, P_{30} and k_T are considered as constants (independent of volume of liquid in the mixing cell, V), while the parameters C_1, P_{10} and P_{13} are forced to be linear functions of V in agreement with the constancy in the injection flow. This builds on that to observe the evolution of the static and dynamic response of the calorimeter (sensitivity and time constants) is necessary to assume different invariants (one for each level of liquid). This approach is valid to describe the operation of the calorimeter and reflects the experimental reality when both flow injection [10, 11] and the duration of injection pulses (in our case, 1 μL s^{-1} for 100 s) is decreasing. The results of the identification process are shown in Tables 1 and 2.

Figure 3 shows the calculated and experimental curves and their corresponding powers. In the calculation, we have corrected the baseline of each experimental curve excluding, in this process of identification, the power dissipated by the stirrer. The electric power dissipated is a known quantity because it has been measured experimentally but the mixing power, associated with each injection pulse, is supposed to have a rectangular shape and that its duration is equal to the injection time. The mixing power for each pulse of injection is determined from the enthalpies of mixing obtained for each experimental curve [17]. The output of the system to the power dissipated by the stirrer is further studied, checking the consistency between the experimental curve and those obtained by the model. For example, for a stirring of 120 rpm and a volume of 1.5 mL of 2-pyrrolidone, a constant power of 0.352 mW (Fig. 4) is dissipated. Figure 5 shows enlargements for Fig. 4 and for the injection pulse (M5) in Fig. 3. In Fig. 5, the agreement between the experimental curves and those calculated by the model can be observed.

Table 2 also shows the parameters of the different TF for each value of C_1, P_{10} and P_{13}. Since the static response of the system is given by the sensitivity and it depends on the volume placed in the mixing cell, we calculate the sensitivities by averaging the values listed in the table. The sensitivity values obtained were $K_{\text{mix}} = 396 \pm 11$ mV W^{-1} and $K_{\text{Joule}} = 347 \pm 3$ mV W^{-1}. Moreover, as the dynamic response of the system is given by the time constants, we

Table 2 Values calculated for variable parameters of the RC model and for the characteristic parameters of the transfer functions (Eq. 3)

V/mL	C_1/J K^{-1}	P_{10}/W K^{-1}	P_{13}/W K^{-1}	τ_1/s	τ_2/s	τ_3/s	τ^*_{Joule}/s	τ^*_{mix} (s)	K_{Joule}/mV W^{-1}	K_{mix}/mV W^{-1}
1.5	3.2106	0.00364	0.01166	278.6	130.4	18.6	153.1	15.5	349.7	384.7
1.6	3.4320	0.00381	0.01296	281.7	128.1	18.6	152.3	15.8	349.2	388.8
1.7	3.6534	0.00398	0.01426	284.8	125.9	18.6	151.6	16.1	348.6	392.4
1.8	3.8748	0.00416	0.01556	287.7	123.9	18.6	151.0	16.3	348.1	395.4
1.9	4.0962	0.00433	0.01685	290.7	122.0	18.6	150.4	16.5	347.5	397.9
2.0	4.3176	0.00451	0.01815	293.5	120.2	18.6	149.9	16.7	346.9	400.1
2.1	4.5390	0.00468	0.01945	296.4	118.5	18.6	149.5	16.9	346.3	402.0
2.2	4.7604	0.00486	0.02075	299.2	116.9	18.6	149.1	17.0	345.8	403.6
2.3	4.9818	0.00503	0.02204	301.9	115.4	18.6	148.7	17.1	345.2	405.0
2.4	5.2032	0.00521	0.02334	304.6	113.9	18.6	148.4	17.3	344.6	406.2
2.5	5.4246	0.00538	0.02464	307.3	112.5	18.5	148.1	17.4	344.0	407.2

V is the volume of liquid in the mixing cell

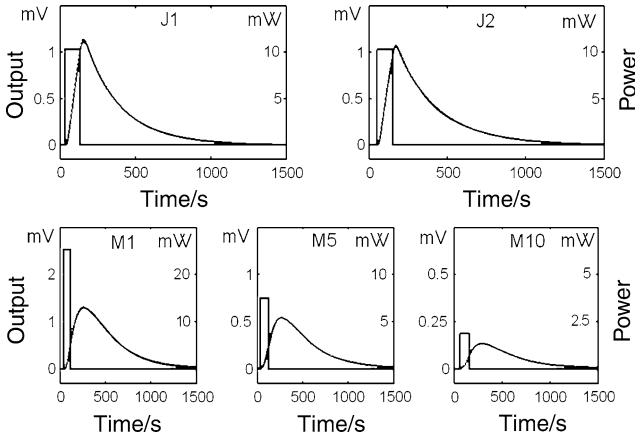

Fig. 3 Details concerning the identification process model (simultaneous adjustment of the calorimetric curves J1, J2, M1, M5 and M10 in Fig. 2). The power dissipated, $w(t)$, is expressed in mW. The calorimetric outputs, $y(t)$, and those calculated by the model are expressed in mV

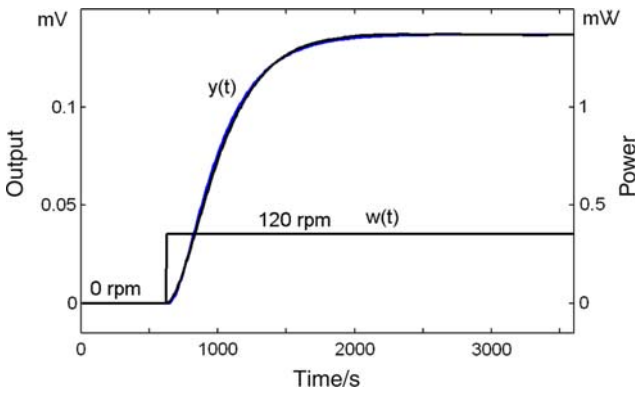

Fig. 4 Evaluation of the stirring power (0.352 mW) using the RC model: The power dissipated, $w(t)$, is expressed in mW. The calorimetric output, $y(t)$, and those calculated by the model, $y_{\text{cal}}(t)$, are expressed in mV. In the experiment, the mixing cell contains 1.5 mL of 2-pyrrolidone and the stirring speed changes from 0 to 120 rpm

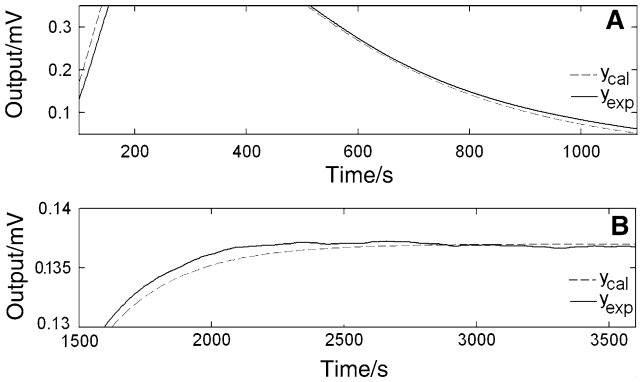

Fig. 5 Graphic detail showing the agreement between the experimental curves and those calculated using the model. **a** Expansion of the M5 curves in Fig. 3. **b** Enlargement of the curves in Fig. 4

compared the dynamics of the different TF through the representation of their magnitudes versus frequency (Fig. 6). The figure shows that the response to an electric dissipation is faster than to a mixing dissipation. Moreover, since there are also differences between the dynamics of the initial and final situations of the injection process, we have expanded the area of Fig. 6, corresponding to the very low frequencies, Fig. 7, in which it can be observed that the response system is slower when increasing the volume of liquid in the mixing cell.

Simulation and results

This section presents the results obtained from the simulation, focusing on two aspects: (i) the effect of the injection and (ii) the change of the baseline. Generally, the contribution due to these effects is relatively small (around 2% of the heat of mixing), however, when the heat of mixing is small ($\approx$0.5 J) then these effects must be evaluated to determine this energy with higher accuracy.

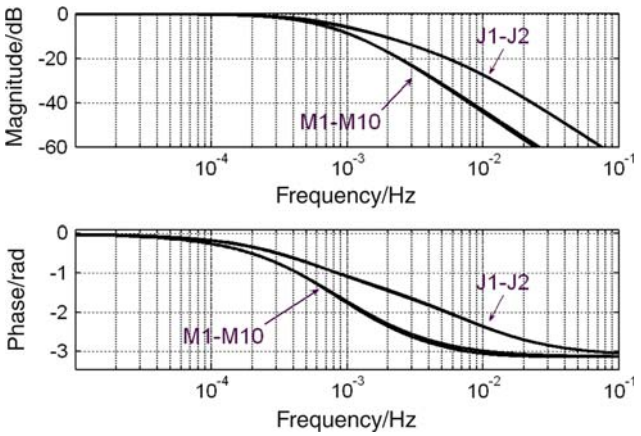

Fig. 6 Variation of magnitude (in dB) and phase (in rad) for the normalized transfer functions, TF(*jw*)/TF(0), versus frequency for the process corresponding to J1–J2 and M1–M10. Magnitude (in dB) = 20 $\log_{10}$ (Magnitude)

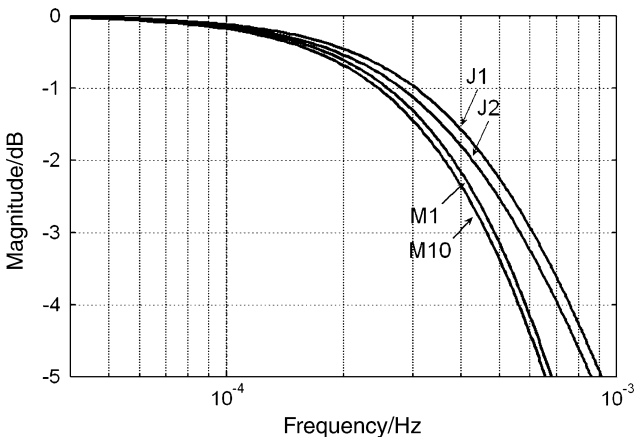

Fig. 7 Magnitude (in dB) of transfer functions. The graph shows an expansion of the zone of very low frequency in Fig. 6

As noted in the "Introduction" section of this article, the effect of the injection is associated with the change in temperature of the liquid when it passes from the thermostat to the mixing cell. Furthermore, the power associated with this process has the opposite sign of the mixing power. In fact, when the mixture is exothermic: $T_1 > T_0$, $W_{mix} > 0$ and $\rho c_p f(T_0–T_1) < 0$. On the contrary, when the mixture is endothermic: $T_1 < T_0$, $W_{mix} < 0$ and $\rho c_p f(T_0–T_1) > 0$. In order to show experimentally this effect, the following experiment was carried out: A Joule dissipation is caused. When the calorimetric output reaches stationary state, a liquid is injected on a known quantity of the same liquid, decreasing then the calorimetric output. Once the injection has ceased, the calorimetric output returns to its initial value.

Figure 8 shows the simulation of a specific measure to assess this effect. Injecting a liquid with values of $\rho c_p f = 0.0022$, 0.0044 and 0.0066 W K^{-1} corresponds to

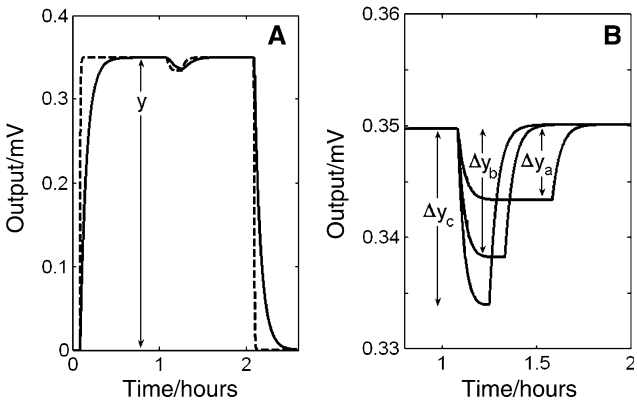

Fig. 8 Evaluation of the effect of injection. Simulation of Joule dissipation and an injection in the middle of it. **a** The calorimetric output (*solid line*) and the filtered curve (*dashed line*). **b** An extension of the area for three injection flows: $\Delta y_a = 6.3$ μV; $\Delta y_b = 11.5$ μV; $\Delta y_c = 15.8$ μV, for $f_a = 1$ μL s^{-1}, $f_b = 2$ μL s^{-1} and $f_c = 3$ μL s^{-1}

the injection flows $f = 1$, 2 and 3 μL s^{-1}. In this way, the injected volume was 1.8 mL. The decrease of the signal (Δy) is best determined when two derivative filters and an integrator filter $(1 + s\tau_1) \cdot (1 + s\tau_2)/(1 + s\tau^*)$ are applied to the calorimetric signal [18], and, to evaluate the effect of the injection, the decrease of the signal is divided by the value of the calorimetric signal corresponding to the stationary state: ($\Delta y/y$). Thus, the effect of the injection for each flow, and for a liquid with $\rho c_p = 2.2$ $JK^{-1}mL^{-1}$, is the following: 1.8, 3.3 and 4.5%. These results are consistent with those obtained experimentally in a previous study [3].

When the heat of mixing is very small and changes in the stirring power are produced as a result of changes in the physical properties of the mixture, during the injection, relatively large disturbances in the baseline can occur. This situation is given, for example, when the formamide + ethanediol binary system is experimentally studied [6]. Figure 9a shows the calorimetric signal corresponding to two injection pulses of 50 μL of formamide ($f =$ 1 μL s^{-1}) on 1 mL of ethanediol. When the second pulse occurs, a negative jump of 20.5 μV in the baseline is produced. On the other hand, when the mixing energy is obtained using a curve, whose baseline has been previously corrected, the mixing energy is 80 mJ; however, if a derivative filter is applied to the experimental curve and later the baseline is corrected, the mixing energy is 94 mJ, which means an increase of 17.5% (both cases are shown in Fig. 9b). For this reason, it is always better to work with a signal in which part of the inertia of the device (given by the time constants of the TF) has been previously removed.

Aiming to show the situation described above, we simulated an experiment involving injecting a liquid ($\rho c_p = 2.2$ J $K^{-1}mL^{-1}$) for 100 s with a flow of 1 μL s^{-1}, which produces a mixing energy of 150 mJ. In the

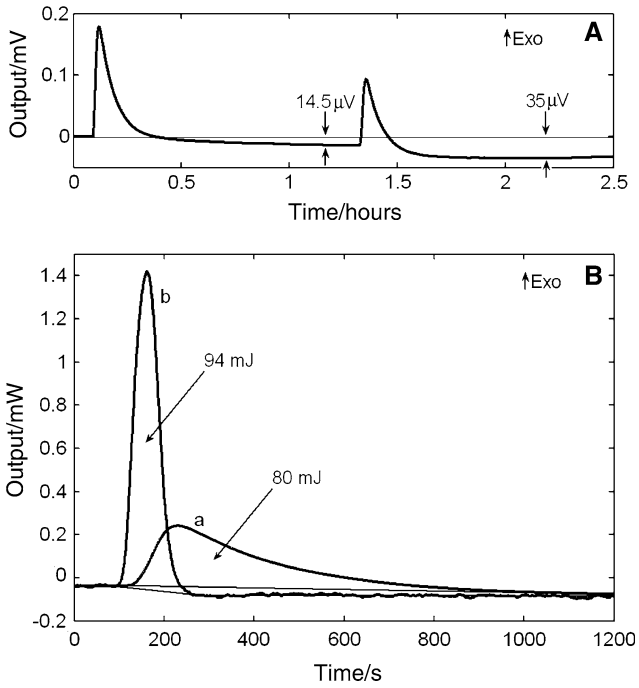

Fig. 9 **a** Experimental ITC curve for two injection pulses of 50 µL of formamide ($f = 1$ µL s^{-1}) on 1 mL of ethanediol. **b** Energy of the second injection pulse. Comparison between the values obtained from ITC curve (**a**) and from the filtered signal with a time constant (**b**)

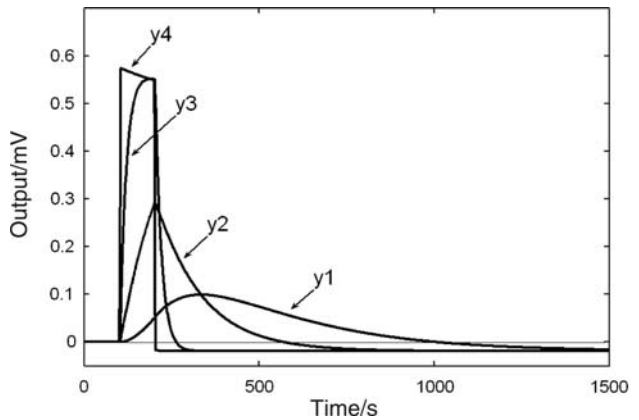

Fig. 10 Simulation of a mixture dissipation (150 mJ) with a flow injection of 1 µL s^{-1} for 100 s, where a change in the level of baseline is observed. Curves y_2, y_3 and y_4 are the result of applying a filter to the calorimetric signal (y_1). See Table 3

simulation, a reduction of 50 µW in the stirring power has been caused, resulting in a decrease in the level of the baseline (Fig. 10). The mixing energy for the four curves (the calorimetric signal and those that result from applying the filters specified in Table 3), shown in Fig. 10 were previously obtained by correcting the baseline. Subsequently, the effects due to injection were corrected, and, finally, each result was divided by the sensitivity of the calorimeter. The results shown in Table 3 reveal that it is

Table 3 Results obtained in the simulation for the heat of mixing (Fig. 10)

Curve	Applied filter	Area/mJ	Error/%
y_1	None	106.12	29.3
y_2	$(1 + s\tau_1)$	126.36	13.8
y_3	$(1 + s\tau_1)\ (1 + s\tau_2)$	147.16	1.9
y_4	$(1 + s\tau_1)\ (1 + s\tau_2)\ (1 + s\tau_3)/(1 + s\tau^*_{mix})$	149.49	0.3

necessary to apply at least two derivative filters to obtain the mixing energy with an error <2%. The time constants used for the filters applied were those that correspond to the volume of liquid in the mixing cell, in accordance with the identification made (Table 2).

Conclusions

In this article, a model designed to describe the operation mode of an ITC is obtained. The model allows the carrying out of a quantitative analysis for several thermal effects that occur when a liquid is injected on another to determine heat of mixing. These effects are experimentally observed and their correction is necessary in some cases.

The effect due to injection is proportional to the injection flow and the heat capacity of the injected liquid. Although in the simulated case this effect is around 1.8%, if a liquid (like water) with a higher heat capacity was injected, the effect would be doubled (3.6%).

Methods for correcting the baseline, when a relatively large one is produced in it, have been developed. In the case studied by the simulation, it is shown that if the baseline is not corrected after an appropriate filtering of the signal, the mixing heat is determined with an error of 29%.

The proper correction of the baseline involves applying derivative filters and/or integrating them in the calorimetric signal. The time constants values to be used for these filters should be the same as in the experimental system. These values are those obtained for the different liquid volumes through modelling.

References

1. Rey C, Rodríguez JR, Pérez-Villar V, Ortín J, Torra V, Dubes JP, et al. Thermogenesis—identification and deconvolution in microcalorimetric systems with continuous injection for the study of liquid-mixtures. Thermochim Acta. 1984;81:97–103.
2. Rodríguez de Rivera M, Tachoire H, Torra V. Calorimetric equipment with time-evolution parameters measurements and modeling in flow and mass-varying calorimetry. J Therm Anal. 1994;41:1385–92.

3. Rodríguez de Rivera M, Socorro F. Injection effect on the sensitivity in an isothermal titration calorimeter. J Therm Anal Calorim. 2006;85:477–9.
4. Socorro F, Rodríguez de Rivera M, Dubès JP, Tachoire H, Torra V. Computer-controlled experimental set-up and signal-processing in calorimetric studies of liquid-mixtures. Meas Sci Technol. 1990;1:1285–90.
5. Rodríguez de Rivera M, Socorro F, Matos JS. Study of the stirring effect in a TAM2277-205 isothermal titration calorimeter. J Therm Anal Calorim. 2008;92:79–82.
6. Rodríguez de Rivera M, Socorro F, Matos JS. Heats of mixing using an isothermal titration calorimeter: associated thermal effects. Int J Mol Sci. 2009;10:2911–20.
7. Rodríguez de Rivera M, Socorro F. Signal processing and uncertainty in an isothermal titration calorimeter. J Therm Anal Calorim. 2007;88:745–50.
8. Rodríguez de Rivera M, Socorro F. Baseline changes in an isothermal titration microcalorimeter. J Therm Anal Calorim. 2005;80:769–73.
9. Isalgue A, Ortin J, Torra V, Viñals J. Heat flux calorimeters: Dinamical model localized time constants. Anales de Física. 1980;76:192–6.
10. Marco F, Rodríguez de Rivera M, Ortín J, Serra T, Torra V. Signal-processing in time-varying calorimeters for the study of continuous liquid-mixtures. Thermochim Acta. 1986;107:149–62.
11. Rodríguez de Rivera M, Socorro F, Dubes JP, Tachoire H, Torra V. Microcalorimetry—identification and automatic deconvolution using physical models. Thermochim Acta. 1989;150:11–25.
12. Socorro F, Rodríguez de Rivera M, Jesús Ch. A thermal model of a flow calorimeter. J Therm Anal Calorim. 2001;64:357–66.
13. Kirchner R, Rodríguez de Rivera M, Seidel JM, Torra V. Identification of micro-scale calorimetric devices. Part VI: an approach by RC-representative model to improvements in TAM microcalorimeters. J Therm Anal Calorim. 2005;82:179–84.
14. Socorro F, Rodríguez de Rivera M. Modellization of the spatial localization effect of the mixture dissipation on the sensitivity in a flow microcalorimeter. J Therm Anal Calorim. 2006;84:285–9.
15. Nelder JA, Mead C. A simplex method for function minimization. Comput J. 1965;7:308–13.
16. The MathWorks, Inc. Optimization Toolbox™ User's Guide, 5th printing. Revised for Version 3.0 (Release 14), June 2004.
17. Tachoire H, Torra V. Thermokinetics by heat-conduction calorimetry. Thermochim Acta. 1987;110:171–81.
18. Marco F, Rodríguez de Rivera M, Ortín J, Serra T, Torra V. A frequential analysis of the numerical algorithms used for inverse filtering in calorimetry. Thermochim Acta. 1986;102:173–8.